

Rheology of non-Brownian Particles Suspended in Concentrated Colloidal Dispersions at Low Particle Reynolds Number

Colin D. Cwalina and Norman J. Wagner

*Department of Chemical and Biomolecular Engineering
Center for Molecular Engineering and Thermodynamics
University of Delaware
Newark, DE 19716*

Submitted to: Journal of Rheology 8/3/2015

Synopsis

The shear flow of non-Brownian glass spheres suspended in a concentrated colloidal dispersion that exhibits non-Newtonian rheology is investigated. At low volume fractions, the addition of non-Brownian spherical particles to the colloidal dispersion leads to an increase in the shear viscosity as well as the dynamic moduli. The flow curves of these suspensions are qualitatively similar to the suspending colloidal dispersion medium, and as such, in this semi-dilute regime, the suspension data can be shifted on to that of the colloidal dispersion medium at constant shear stress with shift factors comparable to those for spherical particles in a Newtonian fluid. At higher volume fractions of non-Brownian spheres, the flow curves change qualitatively and the shear thickening power law exponent becomes an increasing function of particle volume fraction. This increase in the shear thickening power law exponent is shown to be consistent with the effects of confinement on the shear thickening colloidal dispersion and arises from the packing of the larger, non-Brownian particles.

Introduction

Rigid spherical particles immersed in a fluid acquire translational and rotational motion as a result of an imposed bulk laminar shear flow. The flow between particles in a shear field is complex as compared to laminar shear flow; however, if the fluid is Newtonian, a universality in the flow behavior exists such that the suspension viscosity at low particle Reynolds number becomes independent of the particle size and size distribution and only a function of the volume

fraction [Mewis and Wagner (2012)]. Einstein (1911) calculated the particle contribution to the viscosity in the dilute limit as the linear term in an expansion in particle volume fraction:

$$\eta_r = 1 + 2.5\phi + k_2\phi^2 \quad (1)$$

where η_r is the relative viscosity of the suspension and ϕ is the volume fraction of spherical particles. Beyond the dilute limit additional terms are needed to account for the contribution of particle interactions to the viscosity. For the case of a randomized microstructure, Batchelor and Green (1972) calculated the value of k_2 to be 5.2 for monodisperse hard spheres, which was later refined to a value of 5.0 by Wagner and Woutersen (1994). A plethora of models have been proposed for more concentrated suspensions [Faroughi and Huber (2015)]. In particular, the semi-empirical model of Morris and Boulay (1999) can correlate the measured and simulated viscosity and normal stress differences, with coefficients recently reported by Cwalina and Wagner (2014). Including Brownian motion introduces a time scale and the viscosity becomes dependent on the Péclet number, such that the low and high shear viscosities, as well as the viscosity in the shear-thickened state can be defined [Brady and Morris (1997)] and are successfully described by semi-empirical models [Russel *et al.* (2013); Cwalina and Wagner (2014)]. This very brief introduction is meant to show that extensive research has mapped out the rheological properties of suspensions of hard spheres in Newtonian fluids with and without Brownian motion, although much remains to be determined concerning the effects of size polydispersity, particle shape, the presence of any additional interparticle interactions such as friction [Mari *et al.* (2014)], particle inertia [Haddadi and Morris (2014)], as well as the effects of shear-induced particle migration and shear banding [Ovarlez *et al.* (2009)].

Many real-world industrial processes involve the flow of suspensions of non-Brownian particles suspended in colloidal dispersions. Concrete—formed by mixing cement with water, sand, and gravel—is the most widely consumed construction material in the world [Aitcin (2000)]. Cement itself is comprised of colloidal particles that exhibit shear thinning and shear thickening rheology [Toussaint *et al.* (2009)]. Highways in the United States are made almost exclusively out of Portland cement concrete along with asphalt and bitumen wearing surfaces [Zapata and Gambatese (2005)]. In the energy sector, concentrated coal-water slurries are being investigated as replacements for petroleum-derived fuels [Mishra *et al.* (2002)]. Transporting these slurries through long pipelines has motivated a recent surge in the study of their non-Newtonian flow properties [Chen *et al.* (2009)]. Additionally, large quantities of mineral tailings from mining operations must be pumped to disposal facilities where knowledge of non-Newtonian flow behavior is essential for transport optimization [Nguyen and Boger (1998)]. On a more tasteful level, ice cream is formed from a liquid suspension containing tiny ice crystals and fat globules in a syrup of sugars and polysaccharides [Goff (1997)]. These applications are representative of the broad use of suspensions comprised of both Brownian and non-Brownian particles, which will benefit from a basic, quantitative understanding of how the flow properties of a non-Newtonian suspending medium comprised of a colloidal dispersion will be affected by the addition of non-Brownian spherical particles.

Despite comprising some of the most significant materials used by man in terms of mass and volume, there is a notable absence in the literature of systematic studies of model suspensions of non-Brownian particles in shear thickening colloidal dispersions. Liard *et al.* (2014) studied suspensions of $> 50 \mu\text{m}$ glass beads in a shear thickening suspension of cornstarch and water but the cornstarch particles were outside of the colloidal size range. In contrast, there exists significant research into the rheology of suspensions of non-Brownian particles in viscoelastic fluids, such as polymer and surfactant solutions and polymer melts (for a review see Mewis and Wagner (2012)). The non-Newtonian nature of the suspending fluid has been shown to directly affect particle motion [Slattery and Bird (1961); Karnis and Mason (1966); Gauthier *et al.* (1971); D'Avino *et al.* (2008); D'Avino *et al.* (2008); Snijkers *et al.* (2009)]. The fore-aft symmetry between two approaching particles is lost [Fabris *et al.* (1999)], which can lead to a number of surprising microstructural changes for dilute suspensions under shear flow, including particle chaining [Michele *et al.* (1977); Lyon *et al.* (2001); Scirocco *et al.* (2004)]. With regards to shear thickening colloidal dispersions, a recent report documents the rheological and morphological properties of “suspoemulsions”, where at high colloidal dispersion concentrations the multiphase fluid can exist as an emulsion suspended in a colloidal, shear-thickening fluid [Fowler *et al.* (2014)]. There, the presence of dispersed emulsion droplets of low viscosity oil within the colloidal dispersion systematically shifts the mixture’s non-Newtonian shear rheology. One important observation from that work is that the shear thickening transition for the suspoemulsions scales more closely with the applied shear stress than the shear rate.

Direct numerical simulation results for spherical particles suspended in viscoelastic media are available for a number of constitutive models for the suspending fluid, but such simulations are generally limited to investigating the detailed motion of a small number of particles. The large disparity in time and length scales required for a direct particle simulation of a suspension of non-Brownian spheres in a dispersion of Brownian spheres that properly includes hydrodynamic interactions is beyond current computational capabilities [Flatt *et al.* (2004)]. Note that such systems cannot be merely viewed in terms of particle size polydispersity. The treatment of a suspension of non-Brownian particles mixed with Brownian particles requires simulating particles separated by an order of magnitude or more difference in length scales, which translates into three orders of magnitude in mass for equivalent densities. The effect of mixing binary size mixtures of colloidal particles is well understood in terms of hydrodynamic effects [Bender and Wagner (1996)], whereas binary mixing of non-Brownian particles is also well understood in terms of the dependence on the maximum packing fraction [Chong *et al.* (1971); Shapiro and Probstein (1992)].

Remarkably, despite the complex local flows between particles, a plethora of experimental evidence shows the bulk viscosity of suspensions of non-Brownian spherical particles in viscoelastic fluids largely reflects the non-Newtonian viscosity of the suspending medium, and as a result, scaling laws have been proposed. Early work on polymer solutions by

Highgate and Whorlow (1970) first suggested that relative fluidities of suspensions could be scaled onto that of the suspending fluid with simple shift factors over a wide range of particle fractions. Additional authors [Mewis and de Bleyser (1975); Kataoka *et al.* (1978); Chan and Powell (1984); Metzner (1985); Poslinski *et al.* (1988); Malkin (1990); Aral and Kalyon (1997); Zarraga *et al.* (2001)] investigated other types of viscoelastic suspending fluids and observed similar behavior. Using an effective shear rate concept, Ohl and Gleissle (1993) formalized a general shifting procedure to shift suspension data onto that of the suspending medium at constant shear stress:

$$\text{Shift Factor} = \frac{\dot{\gamma}(\phi=0)}{\dot{\gamma}(\phi)} \Big|_{\sigma} = \frac{\eta(\phi)}{\eta(\phi=0)} \Big|_{\sigma} \quad (2)$$

This shifting procedure works remarkably well to collapse suspension data across a broad range of volume fractions and for various types of viscoelastic media. It is important to note that the premise for this shifting procedure is the treatment of the viscoelastic medium as a continuous fluid phase. Although not formulated specifically for analyzing suspensions of non-Brownian particles in colloidal dispersions, this body of literature provides a possible framework in the absence of other theories.

In the present work, we explore and report on the shear flow behavior of non-Brownian spherical particles suspended in model, non-Newtonian colloidal dispersions. This particular choice of suspending medium is of particular interest in that colloidal dispersions exhibit a rich shear-rate dependent rheology that includes a zero-shear viscosity [Russel *et al.* (2013)], viscoelasticity [Shikata and Pearson (1994)], shear thinning, a high-shear viscosity plateau, and shear thickening at high shear rates [Laun (1984); Cwalina and Wagner (2014)]. In this study, the non-Brownian and colloidal particles are separated by more than order of magnitude in size and more than three orders of magnitude in mass. As such, we explore treating the colloidal dispersion as a continuous fluid and test the applicability of the viscosity shifting hypothesis of Ohl and Gleissle (1993) to this particular class of suspensions in non-Newtonian fluids. The dynamic moduli and normal stress differences are also investigated and their behavior compared to that observed for suspensions of non-Brownian particles in various other viscoelastic media.

Experimental Section

Rheological Characterization

Rheological measurements were performed on a torque-controlled Discovery Hybrid Rheometer from TA Instruments (New Castle, DE). A 20 mm parallel plate tool was used for steady shear and dynamic oscillatory measurements. A cone and plate tooling was also studied

but difficulties were encountered due to large particle size relative to the truncation gap. In steady shear measurements, the shear stress, σ , was extracted from Equation 3 as:

$$\sigma = \frac{M}{2\pi R^3} \left[3 + \frac{d \ln M}{d \ln \dot{\gamma}_R} \right] \quad (3)$$

where M is the applied torque, R is the plate radius, and $\dot{\gamma}_R$ is the shear rate at the rim of the plate. The difference between the first and second normal stress differences, N_1 and N_2 respectively, was obtained as:

$$N_1 - N_2 = \frac{F_Z}{\pi R^2} \left[2 + \frac{d \ln F_Z}{d \ln \dot{\gamma}_R} \right] \quad (4)$$

where F_Z is the axial thrust on the tool, and $\dot{\gamma}_R$ is the shear rate at the rim. In oscillatory measurements, the dynamic moduli were computed as:

$$G'(\omega) = \frac{2HM \cos \delta}{\pi R^4 \theta} \quad (5)$$

$$G''(\omega) = \frac{2HM \sin \delta}{\pi R^4 \theta} \quad (6)$$

where H is the gap height, δ is the phase angle, and θ is the angular displacement [Morrison (2001)].

Samples were loaded using a force-gap control with a constant rate of 5 $\mu\text{m/s}$ and a maximum allowable axial force of 0.5 N. Frequency sweeps were performed at 1% strain and data acquired over 10 cycles. In steady shear experiments, at a given applied torque, 10 seconds were allowed for equilibration and the viscosity and normal force were recorded over the following 60 seconds. Particle migration can be a significant difficulty in the measurement of non-Brownian suspensions at high shear rates. However, the frequency sweeps and steady flow curves were found to be reversible, indicating that particle migration and sedimentation were negligible on the timescale of our measurements.

Materials

Two different colloidal dispersions consisting of similar particles varying in size were formulated as suspending fluids. The first consisted of silica nanoparticles (Seahostar KE-P10, Nippon Shokubai Co., Tokyo, Japan) dispersed in a polyethylene glycol (PEG) MW=200 (Aldrich Chemical Company, Allentown, PA; $\eta_f = 0.05 \text{ Pa}\cdot\text{s}$, $\rho = 1.12 \text{ g/cm}^3$) solvent. The average particle radius was measured using small angle neutron scattering for the KE-P10 particles and found to be $a = 60 \text{ nm}$, and the particle density determined from densitometry was $\rho_p = 1.89 \text{ g/cm}^3$ [Kalman (2010)]. The second suspending fluid consisted of silica nanoparticles (Seahostar KE-P50, Nippon Shokubai Co., Tokyo, Japan) of radius $a = 260 \text{ nm}$ and particle density, $\rho_p = 1.96 \text{ g/cm}^3$ [Kalman (2010)] in a PEG-200 solvent. The colloidal dispersions were

prepared by roll mixing for one week and the suspending fluid compositions are reported in Table 1.

Table 1. Composition of suspending fluids

Dispersion	WT% Solids	ρ (g/cm³)	ϕ
KE-P10 in PEG-200	0.50	1.41	0.37
KE-P50 in PEG-200	0.54	1.46	0.40

The non-Newtonian behavior of hard-sphere colloidal dispersions is the result of a competition between thermodynamic Brownian forces and hydrodynamic forces resulting from the imposed shear flow that leads to shear-induced changes in the microstructure. This has been extensively characterized for these colloidal dispersions by rheology and small angle neutron scattering under flow [Gurnon and Wagner (2015)]. The appropriate dimensionless group to gauge this competition is the Péclet number (Pe) given by:

$$Pe = \frac{6\pi\eta_s\dot{\gamma}a^3}{kT} \quad (7)$$

where η_s is the viscosity of the suspending fluid, $\dot{\gamma}$ is the shear rate, a is the particle radius, k is the Boltzmann constant, and T is the absolute temperature. In oscillatory measurements, the shear rate can be replaced by the product of the strain amplitude and the frequency ($\dot{\gamma} \rightarrow \gamma_o\omega$). Measurement across a broader range of Pe number was achieved by recognizing that Pe scales as a^3 and that the Brownian stress, and hence elasticity, scales inversely with a^3 [Russel *et al.* (1989)]. Thus, the use of two colloidal dispersions with widely varying particle sizes as suspending fluids enables exploring a broad range of non-Newtonian phenomena associated with near hard-sphere dispersions, namely viscoelasticity at low Pe and shear thickening at large Pe . This also enables probing the effects of size ratio upon the addition of non-Brownian particles. The flow curves of both colloidal dispersions are shown together in Figure 1 as a function of the Pe number. The use of the two different dispersions allowed us to explore the non-Newtonian behavior of near hard-spheres dispersions over 8 orders of magnitude in Pe number within the measurement range of our rheometer and tooling. The KE-P10 in PEG-200 dispersion has measureable viscoelastic moduli while the KE-P50 in PEG-200 dispersion allows exploring the high shear viscosity plateau and shear thickening behavior at higher Pe number. At the largest Pe numbers explored in this study, the viscosity begins to tend toward a plateau value. This plateau in the viscosity is the emergence of the colloidal shear-thickened state, predicted from theory [Brady and Morris (1997), Bergenholtz *et al.* (2002)], and recently confirmed to exist by the experiments of Cwalina and Wagner (2014).

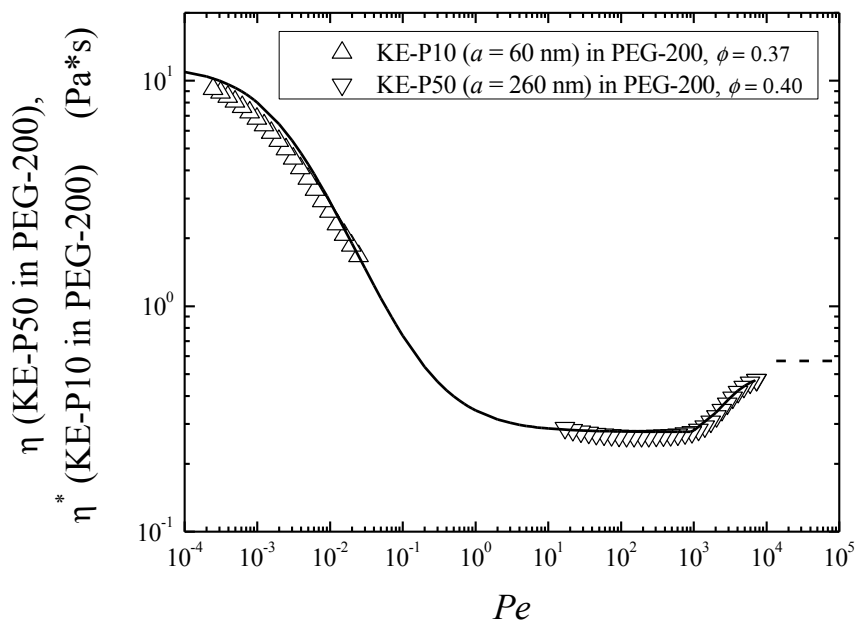


Figure 1. Steady and complex viscosity as a function of the Pe number for the colloidal dispersions used as suspending fluids in this work. The dashed line is the predicted value of the viscosity plateau for a $\phi = 0.40$ near hard-sphere colloidal dispersion [Cwalina and Wagner (2014)]. The solid line is a fit to a modified Cross model given by Galindo-Rosales *et al.* (2011) with model parameters reported in the Appendix.

The non-Brownian spherical particles used in this study were polydisperse ($d_{10} = 5 \mu\text{m}$, $d_{50} = 10 \mu\text{m}$, $d_{90} = 21 \mu\text{m}$) hollow fused borosilicate glass (Spherical[®] 110P8, Potters Industries LLC, Valley Forge, PA) with a manufacturer reported particle density, $\rho_p = 1.10 \text{ g/cm}^3$. The non-Brownian particles (abbreviated “NBP” in subscripts to follow) are nearly density matched to the PEG-200 such that gravitational settling is not a factor on the timescale over which rheological characterization takes place. The non-Brownian particles have an average diameter 20 times that of the KE-P50 particles and are 4000 times more massive. Additionally, they are approximately 80 times larger and 300,000 times more massive than the KE-P10 particles. Suspensions were prepared by the addition of the non-Brownian particles to the colloidal dispersions and roll mixing for one week. Suspensions were formulated by weight and the volume fractions calculated using the measured densities. Throughout the remainder of this paper, the volume fraction of non-Brownian particles, ϕ_{NBP} , is calculated as the volume of non-Brownian particles divided by the total volume of the suspension, noting that the volume fraction of the colloidal particles in the suspending liquid medium remains constant. The suspension compositions studied are reported in Table 2.

Although the particles were nearly neutrally buoyant, particle inertia can create shear thickening for a particle Reynolds number (Re_p) on the order of 10^{-1} or larger [Kulkarni and Morris (2008)]. The particle Reynolds number is defined using the particle radius as the relevant length scale:

$$Re_p = \frac{\dot{\gamma} a^2 \rho}{\eta_s} \quad (8)$$

During rheological measurement, the largest particle Reynolds number encountered in any of the suspensions was on the order of 10^{-3} so particle inertia was not a contributing factor to the measured suspension viscosity.

Table 2. Suspension compositions used in this study.

Suspending Fluid: KE-P10 ($a = 60$ nm) in PEG-200 ($\phi = 0.37$)					
Suspension	WT% NBP	ρ (g/cm³)	ϕ_{NBP}	$\phi_{\text{KE-P10}}$	$\phi_{\text{Total Solids}}$
1	0.04	1.41	0.05	0.35	0.40
2	0.08	1.40	0.10	0.33	0.43
3	0.12	1.38	0.15	0.31	0.46
Suspending Fluid: KE-P50 ($a = 260$ nm) in PEG-200 ($\phi = 0.40$)					
Suspension	WT% NBP	ρ (g/cm³)	ϕ_{NBP}	$\phi_{\text{KE-P50}}$	$\phi_{\text{Total Solids}}$
1	0.03	1.44	0.04	0.39	0.43
2	0.07	1.42	0.09	0.36	0.45
3	0.12	1.40	0.15	0.34	0.49
4	0.30	1.33	0.36	0.26	0.62
5	0.38	1.30	0.45	0.22	0.67
6	0.41	1.29	0.48	0.21	0.69

Results and Discussion

Linear Viscoelastic Regime

Brownian motion within a colloidal dispersion gives rise to viscoelasticity [Shikata and Pearson (1994)] as evidenced by the dynamic moduli of the $\phi = 0.37$ dispersion of KE-P10 in PEG-200 shown in Figure 2. The effect of adding small amounts of non-Brownian spheres is overlaid. At a given frequency, the addition of non-Brownian particles results in a vertical shift of both dynamic moduli curves while the shape of the curve reflects that of the colloidal dispersion as the suspending medium. This result is consistent with measurements of the dynamic moduli in other viscoelastic suspending fluids [Chan and Powell (1984); Schaink *et al.*

(2000); See *et al.* (2000); Le Meins *et al.* (2002); Pasquino *et al.* (2008)]. As non-deformable spherical particles are added to the colloidal dispersion medium, the local strain amplitudes in the colloidal dispersion are, on average, greater than the applied strain amplitudes. Consequently, the dynamic stresses are higher and when divided by the applied deformation, yield higher moduli.

Visual inspection suggests that a single scalar shift should be sufficient to shift the dynamic moduli data onto that of the colloidal dispersion medium and form a master curve. Indeed, such a single vertical shift factor for a given volume fraction of non-Brownian spheres successfully forms a master curve for the dynamic moduli data as shown in Figure 3. Furthermore, the dynamic moduli can be collapsed onto the values of the colloidal dispersion medium with roughly the same shift factor as seen in Figure 4. This result has already been demonstrated for suspensions of non-Brownian spheres in Newtonian fluids where the suspension relative viscosity and elastic modulus have been shown to collapse onto a master curve when plotted against the proximity to maximum packing [Chong *et al.* (1971); Mewis and Wagner (2012)].

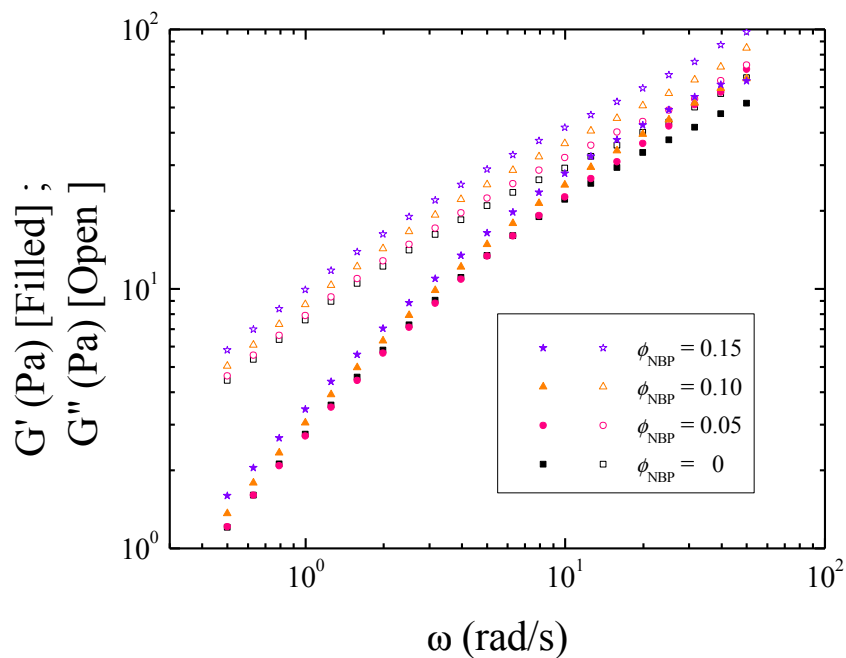


Figure 2. Dynamic moduli of suspensions of non-Brownian glass spheres in a $\phi = 0.37$ KE-P10:PEG-200 colloidal dispersion.

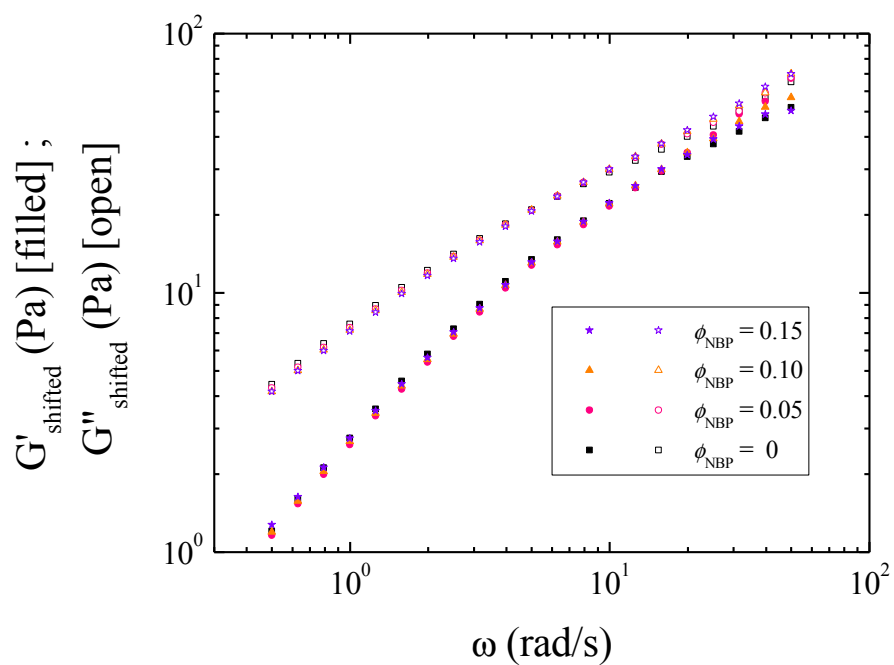


Figure 3. Shifted dynamic moduli curves. Symbols are identical to those used in Figure 2.

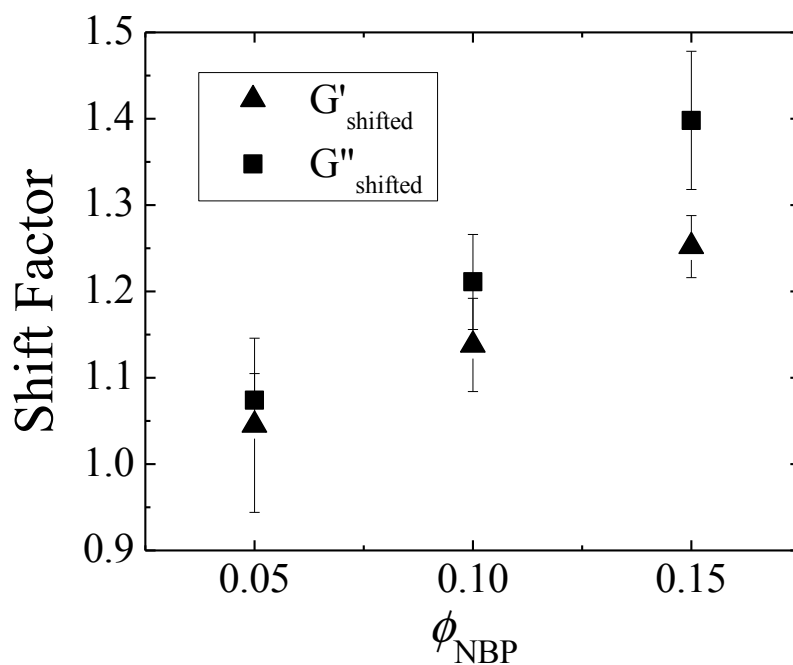


Figure 4. Shift factors required to collapse dynamic moduli data onto that of the colloidal dispersion medium as a function of the volume fraction of non-Brownian spheres.

In Figure 5, the purely hydrodynamic component of the loss modulus ($\omega\eta'_\infty$) has been subtracted off to give only the contribution from Brownian and interparticle interactions, and as such, a characteristic relaxation time can be defined from the crossover frequency. The value of the crossover frequency is shown to be independent of the concentration of non-Brownian particles in this semi-dilute concentration regime. The high frequency viscosity relative to that of the underlying colloidal dispersion medium is plotted as a function of the volume fraction of non-Brownian particles in Figure 7 along with the results expected for non-Brownian particles in a Newtonian fluid. As observed, the high frequency viscosity for these suspensions in a non-Newtonian colloidal dispersion medium can be well approximated by these equations in this semi-dilute concentration regime.

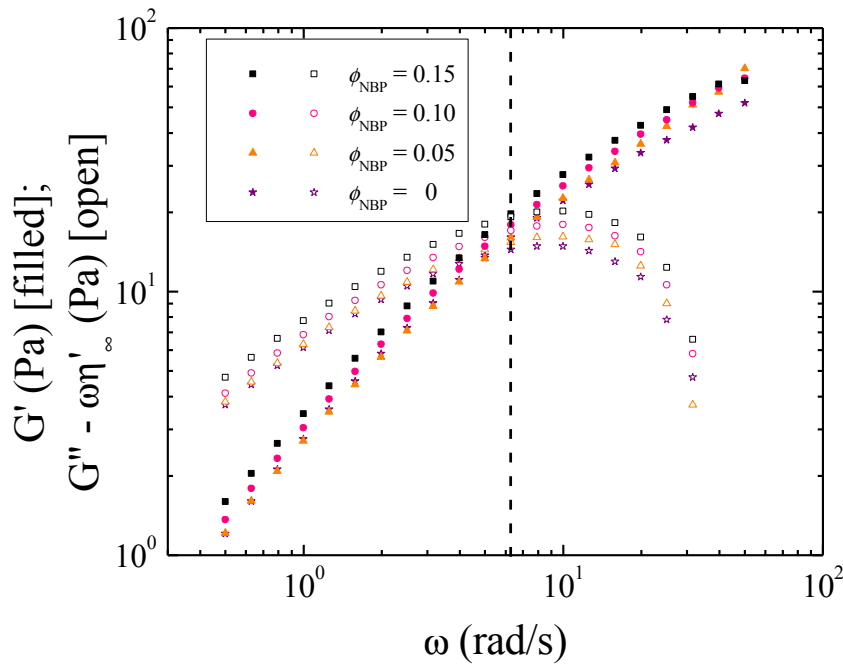


Figure 5. Dynamic moduli of suspensions of non-Brownian glass spheres in a $\phi = 0.37$ KE-P10 in PEG-200 colloidal dispersion with the hydrodynamic component of the loss modulus subtracted off to give the Brownian and interparticle contribution. The dashed vertical line marks the crossover frequency which is independent of the concentration of non-Brownian particles.

High Shear Plateau and Shear Thickening Upturn: Semi-Dilute Regime

To access the high shear plateau and a significant shear thickening regime within the measurement range of the rheometer we studied the same non-Brownian spheres suspended in the colloidal dispersion comprised of the larger KE-P50 ($a = 260$ nm) colloidal particles, also in PEG-200. The viscosity of suspensions at multiple non-Brownian particle volume fractions is displayed in Figure 6.

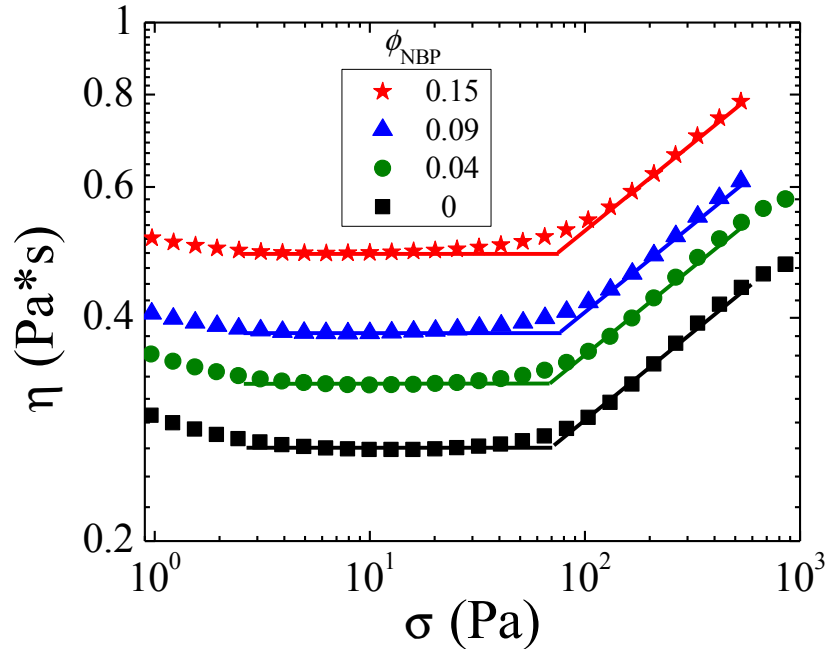


Figure 6. Viscosity of non-Brownian glass spheres suspended in a shear thickening colloidal dispersion of KE-P50 ($a = 260$ nm) particles in PEG-200 as a function of the shear stress. Solid lines are extensions to power law fits to the high shear plateau and shear thickening upturn.

When plotted against the shear stress, the addition of non-Brownian particles shifts the viscosity curves vertically, but parallel, to higher stresses. Note that the exponent of the power law fits to the viscosity in the shear thickening regime remains nearly constant. The critical stress for shear thickening can be defined as the intersection of the high shear plateau with this power law scaling. From Figure 6 it is evident that the onset of shear thickening occurs at a nearly constant value of the shear stress independent of the volume fraction of non-Brownian spheres. The onset of shear thickening in dispersions of spherical colloids is well-established to be stress-controlled [Bender and Wagner (1996); Maranzano and Wagner (2001); Shenoy and

Wagner (2005)], and the data here suggests that the onset of shear thickening in suspensions of non-Brownian particles in these shear-thickening colloidal dispersions is also stress-controlled.

The fact that the onset of shear thickening occurs at the same shear stress regardless of the volume fraction of non-Brownian spheres suggests a reduction of the viscosity curves to a universal behavior using a single, vertical shift factor. Such a reduction is indeed possible as shown in Figure 7, which also plots the shift factor required to achieve a master curve as a function of the volume fraction of non-Brownian particles. These results for the shear viscosity are consistent with the hypothesis of Ohl and Gleissle (1993). This shift factor is the viscosity of the suspension relative to that of the colloidal dispersion medium (a type of relative viscosity) at constant shear stress. As such, it is tempting to compare this relative viscosity to that known for suspensions in Newtonian fluids (given by Equation 1 with $k_2 = 5.0$). To a first approximation, the equations derived for particles in a Newtonian fluid can be used to estimate the viscosity in this concentration regime, although the relative steady shear viscosities measured in this study clearly lie above these predictions. Similar behavior has been observed with suspensions in other viscoelastic media such as Boger fluids [Tanner *et al.* (2013)], silicone oil [Mall-Gleissle *et al.* (2002)], and polydimethylsiloxane [Pasquino *et al.* (2008)] over very similar particle concentrations.

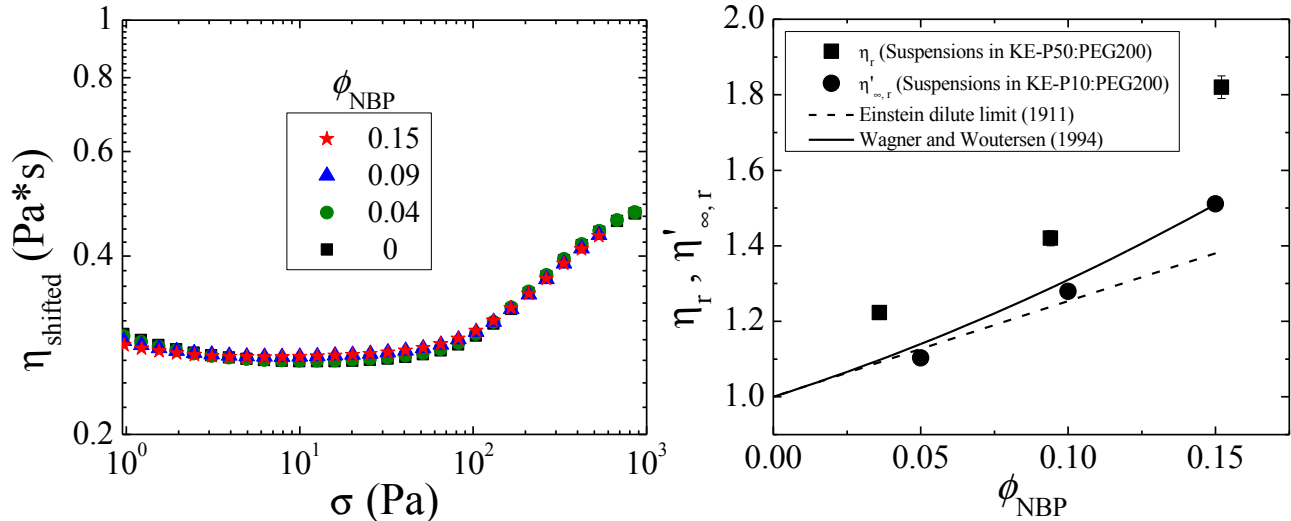


Figure 7. (Left) Shifted viscosity curves for suspensions of non-Brownian spheres in a colloidal shear thickening fluid. (Right) Steady shear (squares) and high frequency (circles) viscosity for suspensions in colloidal dispersion media as a function of the concentration of non-Brownian spheres. The dashed line is the Einstein viscosity equation (Equation 1, $k_2 = 0$) for dilute suspensions of non-Brownian spheres in a Newtonian fluid and the solid line contains the

additional ϕ^2 term of $k_2 = 5.0$ [Wagner and Woutersen (1994)] . Error bars are smaller than data points.

Extension to Higher Particle Concentrations

In Newtonian fluids, at higher particle concentrations, many-body interactions become important to the calculation of the suspension viscosity such that additional higher order terms beyond the ϕ^2 term in Equation 1 are required. The semi-empirical model of Morris and Boulay (1999) has been shown to be successful at describing the viscosity of suspensions of non-Brownian spheres in a Newtonian fluid:

$$\eta_r = 1 + 2.5\phi \left(1 - \frac{\phi}{\phi_{max}}\right)^{-1} + K_s \left(\frac{\phi}{\phi_{max}}\right)^2 \left(1 - \frac{\phi}{\phi_{max}}\right)^{-2} \quad (9)$$

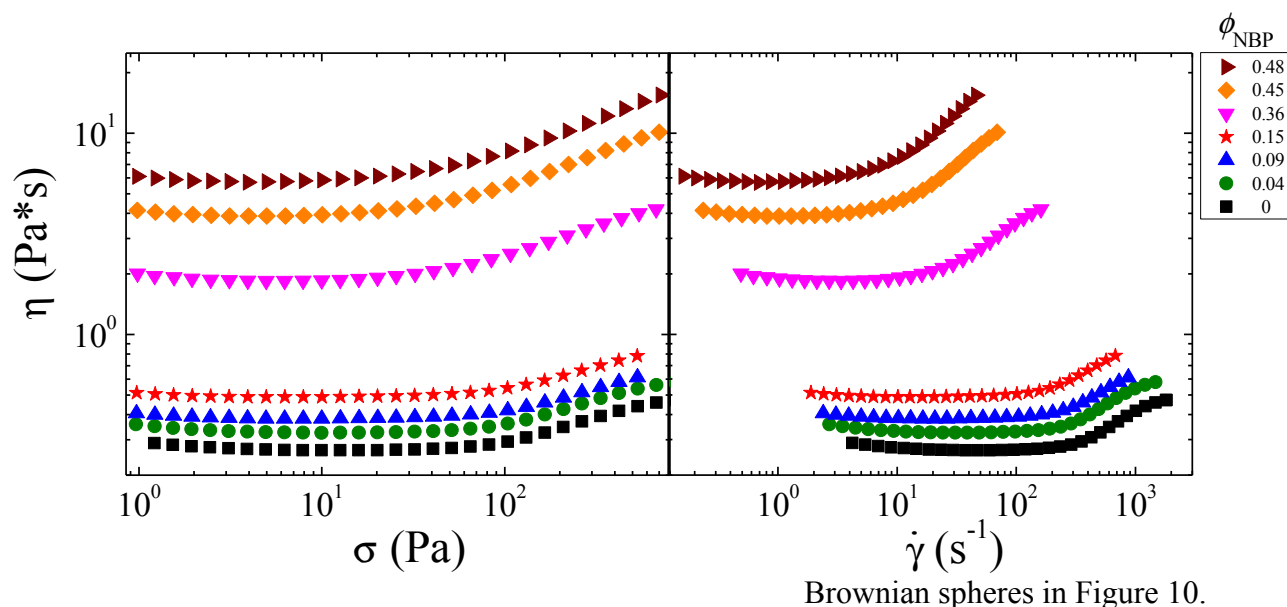
In the equation above, ϕ_{max} is the maximum packing fraction and K_s is a constant.

The flow curves of suspensions containing high volume fractions of non-Brownian spheres are presented in Figure 8 and the model of Morris and Boulay (1999) is applied to the high shear viscosity data in Figure 9. As seen, this semi-empirical model can describe the shift in relative viscosity in the high shear plateau with one adjustable parameter, ϕ_{max} , equal to 0.58 which has been commonly reported as the maximum packing fraction in a number of suspensions of non-Brownian spherical particles in Newtonian fluids [Zarraga *et al.* (2000); Singh and Nott (2003); Boyer *et al.* (2011; Tanner *et al.* (2013)]. This value of ϕ_{max} is below the expected value of 0.638 for random close packing of monodisperse spheres. As our particles are polydisperse, the maximum packing fraction is expected to be larger, and the discrepancy may reflect weak attractive interactions, particle roughness, or particle shape anisotropy. Nonetheless, this model developed for suspensions in Newtonian fluids yields an excellent description of the suspension viscosity data in the high shear plateau at $\sigma = 10$ Pa.

At these higher concentrations of non-Brownian particles, a single, vertical shift factor cannot produce a master curve for all shear stresses and deviations from the shifting procedure become apparent in the shear thickening regime as illustrated in Figure 9. At higher volume fractions of non-Brownian particles, the shear thickening power law exponent of the suspensions appears to increase with the concentration of non-Brownian particles as seen in Figures 8 and 9. Recall that the particle Reynolds number for these suspensions is on the order of 10^{-3} in the shear thickening regime, and as such, particle inertia is not contributing to the measured viscosity. To quantitatively determine the power law exponent, we fit the data for each volume fraction in the range of $\sigma = 100$ to 400 Pa to the power law given by.

$$\sigma = k \dot{\gamma}^n \quad (10)$$

where k is a constant and n is the power law exponent. In this range of shear stresses, all of the dispersions exhibit a power-law shear thickening upturn before the viscosity begins to tend toward the constant viscosity plateau of the shear-thickened state. The shear thickening power law exponent in this regime is shown to be an increasing function of the volume fraction of non-



Brownian spheres in Figure 10.

Figure 8. Flow curves of suspensions of non-Brownian particles in a concentrated colloidal dispersion as a function of the shear stress (left) and shear rate (right).

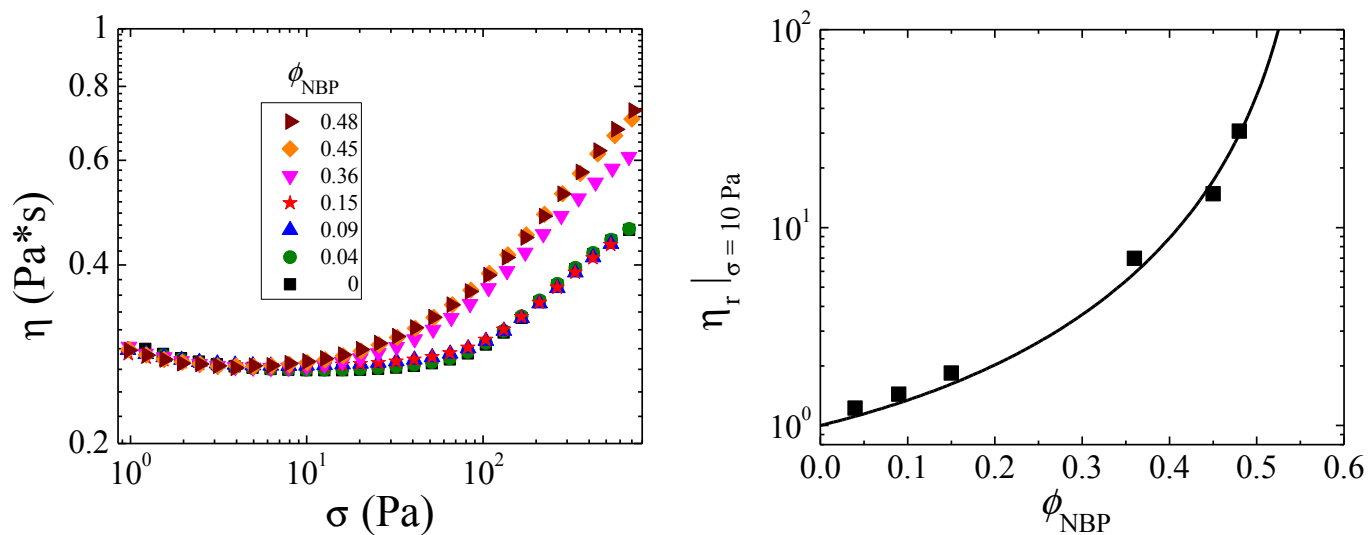


Figure 9. (Left) Viscosity curves for suspensions shifted onto the high shear plateau of the colloidal dispersion medium at $\sigma = 10$ Pa. (Right) Suspension viscosity relative to that of the colloidal dispersion at $\sigma = 10$ Pa. The solid line is a fit of the semi-empirical model of Morris and Boulay (1999) with $K_s = 0.94$.

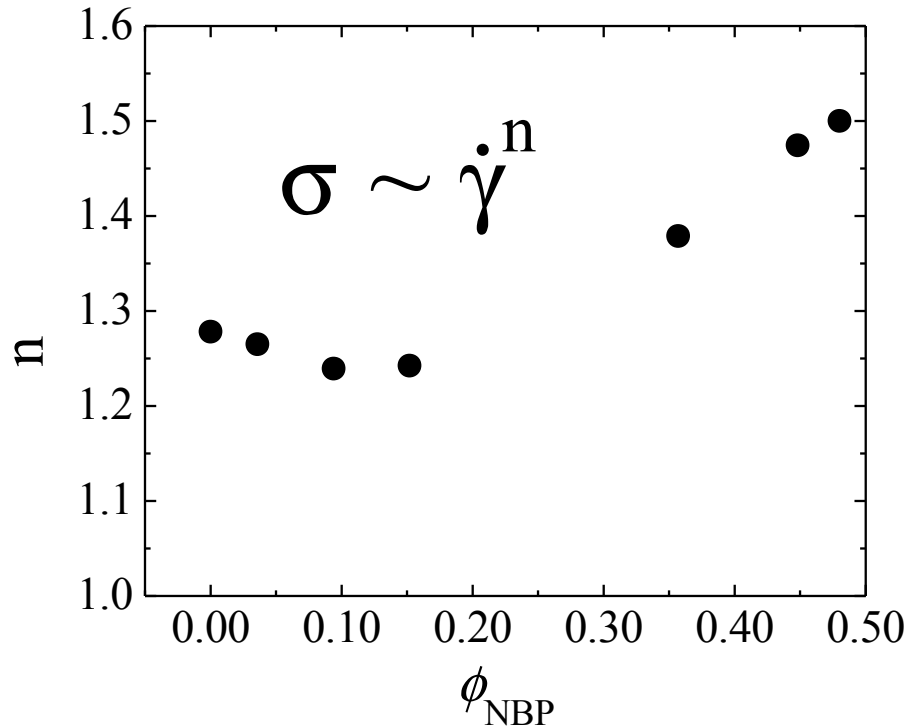


Figure 10. Shear thickening power law exponent as a function of the volume fraction of non-Brownian spheres. Error bars are smaller than data points.

To understand this increase in the shear thickening power law exponent, it is useful to consider the average separation distance between non-Brownian spherical surfaces in suspension as a function of the volume fraction. A simple geometric model as given by [Boersma *et al.* (1990); Bender and Wagner (1996)] yields:

$$\frac{h}{2a} = \left(\frac{\phi_{\text{max}}}{\phi} \right)^{1/3} - 1 \quad (10)$$

where h is the characteristic separation distance of particle surfaces, a is the particle radius, ϕ is the particle volume fraction, and ϕ_{max} is the maximum packing fraction, which is taken to be 0.58 to be consistent with the previous modeling. Figure 11 shows the shear thickening power law exponent as a function of the separation distance between non-Brownian particles (h_{NBP}) normalized by the diameter of the colloidal particles ($2a_{\text{colloids}}$). This parameter physically

represents the number of colloidal particles that could span the characteristic gap between non-Brownian spherical surfaces.

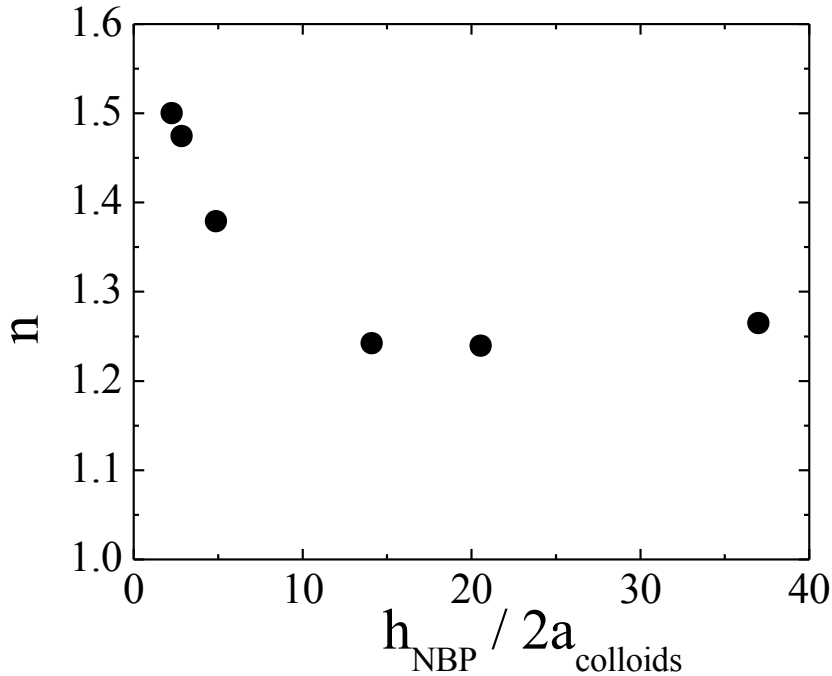


Figure 12. Shear thickening power law exponent as a function of the characteristic separation distance between non-Brownian spheres.

Geometric confinement of a colloidal fluid is known to enhance shear thickening as demonstrated by the narrow-gap Couette measurements of Chow and Zukoski (1995). The change in the shear thickening power law exponent of our suspensions suggests that confinement of the colloidal dispersion medium between non-Brownian spherical surfaces may become relevant when the characteristic gap between the non-Brownian particles becomes on the order of a few colloidal particle diameters. The shear thickening power law exponent in our suspensions remains nearly constant for characteristic separation distances above roughly 15 colloidal particle diameters. Below this spacing threshold, the power law exponent begins to increase. These results are likewise consistent with recent simulation studies of suspensions under confinement by Bian *et al.* (2014). In these simulations, 2-dimensional hydrodynamically interacting particles are sheared between parallel plates. Reducing the plate separation distance below 16 particle diameters was shown to induce formation of hydrodynamic clusters of larger

size, and hence, increase the shear thickening power law exponent. In the present experimental work, at high concentrations, the large non-Brownian spheres provide local confinement of the colloidal particles. Thus, as the colloidal fluid is made to flow between the narrow gaps of non-Brownian spheres at higher volume fractions, it is reasonable to anticipate that this local confinement can promote the formation of larger hydroclusters and stronger shear thickening. Note that this confinement between spherical non-Brownian particles is much less constrained than for parallel plates as in the simulations, and as such, the effects in suspension are not expected to be as dramatic.

Normal Stress Differences

Negative normal stress differences have been reported by authors on a number of suspensions consisting of non-Brownian spheres in Newtonian fluids [Gadalamaria and Acrivos (1980); Zarraga *et al.* (2000); Couturier *et al.* (2011); Dai *et al.* (2013)]. Negative normal stress differences have also been observed for shear thickening in colloidal dispersions, both in Stokesian dynamics simulations [Foss and Brady (2000)] and early experimental measurements [Laun (1994); Lee *et al.* (2006)]. Cwalina and Wagner (2014) recently reported measurements of the first and second normal stress differences for a model shear thickening colloidal dispersion of near hard-spheres. Both N_1 and N_2 were found to be negative in the shear-thickened state with $|N_2|$ slightly larger than that of $|N_1|$ for the most concentrated dispersions. The normal stress differences in colloidal dispersions are a consequence of the highly anisotropic microstructure that develops under flow at high Pe due to lubrication hydrodynamic interactions between particles [Bergenholtz *et al.* (2002)].

An extensive literature also exists for the measurement of normal stress differences in suspensions of non-Brownian spheres in viscoelastic media [Highgate and Whorlow (1970); Mewis and de Bleyser (1975); Chan and Powell (1984); Aral and Kalyon (1997); Zarraga *et al.* (2001); Mall-Gleissle *et al.* (2002); Tanner *et al.* (2013)]. The normal stress differences exhibit power law behavior when plotted against the shear stress on logarithmic axes and shift parallel to each other as the particle concentration is varied. It is important to note that the normal stress differences in these suspensions arise from the elasticity of the underlying suspending fluid whereas the normal stress differences for suspensions in Newtonian fluids are a consequence of viscous hydrodynamic forces between particles.

The difference between the first and second normal stress differences were obtained according to Equation 4 for suspensions of non-Brownian particles in the colloidal dispersion of KE-P50 particles in PEG. For guidance on the expected magnitude of N_1 - N_2 for the colloidal dispersion suspending medium, we used the semi-empirical model of Morris and Boulay (1999) along with the model coefficients determined by Cwalina and Wagner (2014). For systems dominated by hydrodynamic interactions, the normal stress differences are modeled as:

$$\frac{N_1}{\eta_s \dot{\gamma}} = -K_1 \left(\frac{\phi}{\phi_{max}} \right)^2 \left(1 - \frac{\phi}{\phi_{max}} \right)^{-2} \quad (11)$$

$$\frac{N_2}{\eta_s \dot{\gamma}} = -K_2 \left(\frac{\phi}{\phi_{max}} \right)^2 \left(1 - \frac{\phi}{\phi_{max}} \right)^{-2} \quad (12)$$

Combination and rearrangement of Equations 11 and 12 gives:

$$N_1 - N_2 = (K_2 - K_1) \left(\frac{\phi}{\phi_{max}} \right)^2 \left(1 - \frac{\phi}{\phi_{max}} \right)^{-2} \eta_s \dot{\gamma} \quad (13)$$

The values of K_1 and K_2 were reported by Cwalina and Wagner (2014) to be 0.177 and 0.240, respectively, and the limiting behavior of $N_1 - N_2$ in the colloidal shear-thickened state for the $\phi = 0.40$ colloidal dispersion is shown in Figure 12. The shear-thickened state only begins to appear at the highest shear rates probed in this study as the parallel plate tooling limits the maximum shear rate attainable before sample ejection. Nevertheless, at the highest accessible shear rates, the measured values of $N_1 - N_2$ approach the predicted limiting values of the colloidal shear-thickened state.

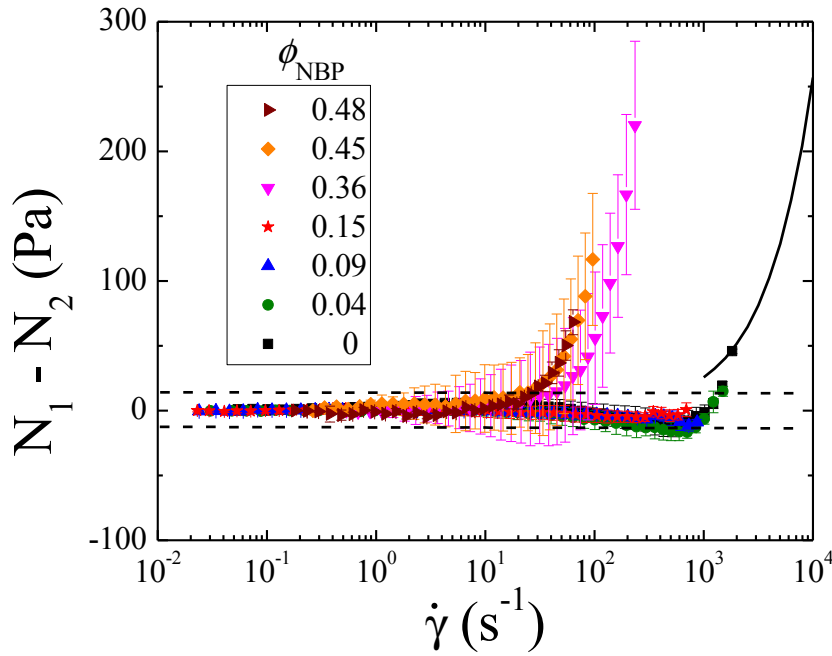


Figure 12. Measurements of $N_1 - N_2$ over a broad range of suspension volume fractions plotted against the shear rate. The solid line is the predicted value of $N_1 - N_2$ for the colloidal dispersion medium ($\phi_{\text{NBP}} = 0$) in the shear-thickened state using the semi-empirical model of Morris and Boulay (1999) and the model coefficients reported by Cwalina and Wagner (2014). The dashed lines mark the resolution of the instrument.

In the semi-dilute regime, the addition of non-Brownian particles does not appreciably alter the values of $N_1 - N_2$ to within instrument resolution. This is consistent with measurements on suspensions in other viscoelastic media where the normal stress differences reflect those of

the underlying suspending fluid. However, at higher volume fractions large positive values of $N_1 - N_2$ are measured that greatly exceed the limiting value for the colloidal fluid in the shear-thickened state and appear at shear rates at least an order of magnitude below that of the colloidal dispersion medium. The measured normal stress differences for the suspensions are shown in Figure 13 plotted logarithmically against the *shear stress* in the spirit of the previous measurements made for suspensions in other viscoelastic media. The normal stress differences for these concentrated suspensions exhibit a power law scaling with the stress and the power law exponent is relatively constant, independent of the concentration of non-Brownian particles. Note that, when plotted against total shear stress, the normal stress differences are much more comparable than when viewed as a function of shear rate. This again highlights the importance of shear stress in controlling the shear thickening behavior of the colloidal dispersion. This normal stress difference increases when non-Brownian particles are added, but the trend when viewed at constant shear stress is not simple. At present, the origin of the normal stress differences in these mixed suspensions is not fully understood and it is not known if the confinement effects that increase the shear thickening viscosity will have a comparable effect on these normal stress differences. Nonetheless, these new measurements on this model system provide data that can be useful for critically testing models and simulations of such mixed suspensions.

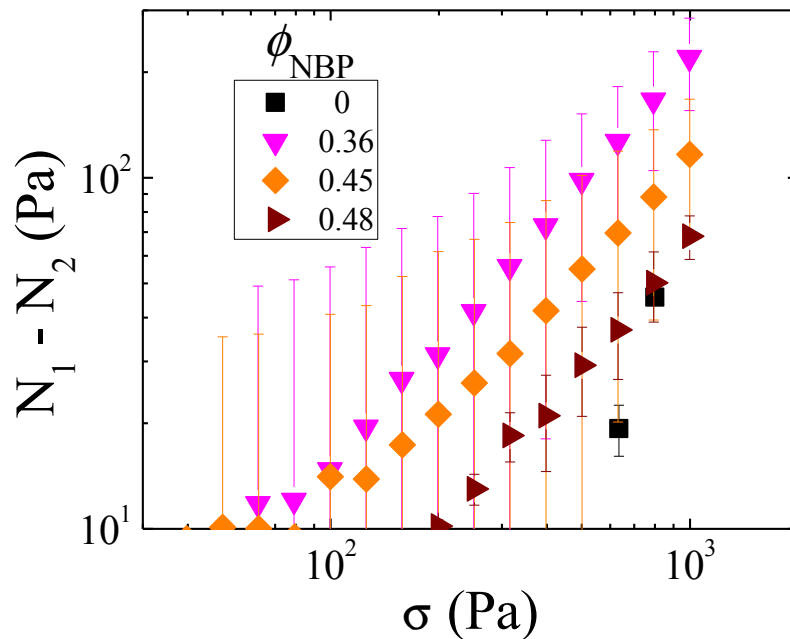


Figure 13. Measured normal stress differences plotted as a function of the shear stress.

Conclusions

Measurements of the dynamic and steady shear rheology of model suspensions of non-Brownian spheres in a non-Newtonian suspending medium comprised of a colloidal shear thickening dispersion are found to strongly reflect the underlying rheological properties of the colloidal dispersion. The linear viscoelastic material functions are found to directly scale with the suspending colloidal dispersion such that the characteristic relaxation time of the suspension remains unchanged upon the addition of non-Brownian spherical particles. In a similar manner, at low volume fractions of non-Brownian spheres, the steady shear viscosity curves in the high shear plateau and shear thickening upturn are found to superimpose through a vertical shift when plotted against the shear stress. This behavior is often reported for suspensions in molecular non-Newtonian fluids and is consistent with the hypothesis of Ohl and Gleissle (1993). Deviations from this simple shifting are observed at higher volume fractions where the shear thickening power law exponent is found to be an increasing function of the concentration of non-Brownian spheres and the normal stress differences are significantly enhanced. This violation of the simple scaling can be attributed to the known effect of confinement on enhancing shear thickening in colloidal dispersions [Chow and Zukoski (1995)].

This experimental investigation of model suspensions of non-Brownian spherical particles in a non-Newtonian colloidal dispersion suspending medium reveals a relatively simple and predictable rheological response for stresses corresponding to the shear thinning regime and high shear plateau of the colloidal dispersion. However, when shear thickening is evident in the colloidal dispersions, local confinement effects become evident at a higher concentration of non-Brownian spheres. Such confinement effects may be even further enhanced in the presence of discontinuous shear thickening colloidal dispersions and future work will address this as well as the role of particle shape.

We note that recent work on novel shear thickening suspoemulsions by Fowler *et al.* (2014) has also shown unanticipated effects in emulsion morphology when the colloidal dispersion is in the shear-thickened state. Previous investigations of non-Brownian particles in non-Newtonian media typically employ shear thinning polymer solutions and melts, wormlike micelles, or Boger fluids where particles have been observed to chain along the flow direction [Michele *et al.* (1977); Lyon *et al.* (2001); Scirocco *et al.* (2004)]. As such, the present work compliments the existing literature reports for suspensions in non-Newtonian media and

motivates a need to further explore the motion of suspended non-Brownian particles in a shear thickening colloidal dispersion.

Acknowledgement

This work was supported by a NASA EPSCoR Grant (NNX11AQ28A) and a Delaware Space Grant Graduate Fellowship (NNX10AN63H).

Appendix

In Figure 1, a modified Cross model is fit to the experimental flow curves. The modification of the Cross model for shear thickening fluids is provided by Galindo-Rosales *et al.* (2011). The best fit model parameters are reported in the table below.

Table A.1. Modified Cross model parameters used in Figure 1.

Parameter	Value
η_0	11.66
η_c	0.28
η_{max}	0.47
n_1	0.36
n_2	0.83
λ_1	$2.13 * 10^7$
λ_2	$3.76 * 10^{-3}$
$\dot{\gamma}_c$	234.45
$\dot{\gamma}_{max}$	1821.17

References

- Aitcin, P. C., "Cements of yesterday and today - Concrete of tomorrow." *Cement and Concrete Research*. **30**, 1349-1359 (2000).
- Aral, B. K. and D. M. Kalyon, "Viscoelastic material functions of noncolloidal suspensions with spherical particles." *J Rheol*. **41**, 599-620 (1997).
- Batchelor, G. K. and J. T. Green, "Determination of Bulk Stress in a Suspension of Spherical-Particles to Order C-2." *Journal of Fluid Mechanics*. **56**, 401-427 (1972).
- Bender, J. and N. J. Wagner, "Reversible shear thickening in monodisperse and bidisperse colloidal dispersions." *J Rheol*. **40**, 899-916 (1996).
- Bergenholtz, J., J. Brady and M. Vucic, "The non-Newtonian rheology of dilute colloidal suspensions." *Journal of Fluid Mechanics*. **456**, 239-275 (2002).
- Bergenholtz, J., J. F. Brady and M. Vucic, "The non-Newtonian rheology of dilute colloidal suspensions." *Journal of Fluid Mechanics*. **456**, 239-275 (2002).
- Bian, X., S. Litvinov, M. Ellero and N. J. Wagner, "Hydrodynamic shear thickening of particulate suspension under confinement." *Journal of Non-Newtonian Fluid Mechanics*. **213**, 39-49 (2014).
- Boersma, W. H., J. Laven and H. N. Stein, "Shear Thickening (Dilatancy) in Concentrated Dispersions." *Aiche Journal*. **36**, 321-332 (1990).
- Boyer, F., E. Guazzelli and O. Pouliquen, "Unifying Suspension and Granular Rheology." *Physical Review Letters*. **107** (2011).
- Brady, J. F. and J. F. Morris, "Microstructure of strongly sheared suspensions and its impact on rheology and diffusion." *Journal of Fluid Mechanics*. **348**, 103-139 (1997).
- Chan, D. and R. L. Powell, "Rheology of Suspensions of Spherical-Particles in a Newtonian and a Non-Newtonian Fluid." *Journal of Non-Newtonian Fluid Mechanics*. **15**, 165-179 (1984).

- Chen, L. Y., Y. F. Duan, C. S. Zhao and L. G. Yang, "Rheological behavior and wall slip of concentrated coal water slurry in pipe flows." *Chemical Engineering and Processing*. **48**, 1241-1248 (2009).
- Chong, J. S., Christia.Eb and A. D. Baer, "Rheology of Concentrated Suspensions." *Journal of Applied Polymer Science*. **15**, 2007-& (1971).
- Chow, M. K. and C. F. Zukoski, "Gap Size and Shear History Dependencies in Shear Thickening of a Suspension Ordered at Rest." *J Rheol*. **39**, 15-32 (1995).
- Couturier, E., F. Boyer, O. Pouliquen and E. Guazzelli, "Suspensions in a tilted trough: second normal stress difference." *Journal of Fluid Mechanics*. **686**, 26-39 (2011).
- Cwalina, C. D. and N. J. Wagner, "Material Properties of the Shear-Thickened State in Concentrated Near Hard-Sphere Colloidal Dispersions." *J Rheol*. **58**, 949-967 (2014).
- D'Avino, G., M. A. Hulsen, F. Snijkers, J. Vermant, F. Greco and P. L. Maffettone, "Rotation of a sphere in a viscoelastic liquid subjected to shear flow. Part I: Simulation results." *J Rheol*. **52**, 1331-1346 (2008).
- D'Avino, G., P. L. Maffettone, M. A. Hulsen and G. W. M. Peters, "Numerical simulation of planar elongational flow of concentrated rigid particle suspensions in a viscoelastic fluid." *Journal of Non-Newtonian Fluid Mechanics*. **150**, 65-79 (2008).
- Dai, S. C., E. Bertevas, F. Z. Qi and R. I. Tanner, "Viscometric functions for noncolloidal sphere suspensions with Newtonian matrices." *J Rheol*. **57**, 493-510 (2013).
- Einstein, A., "A new determination of the molecular dimensions." *Annalen der Physik*. **34**, 591-592 (1911).
- Fabris, D., S. J. Muller and D. Liepmann, "Wake measurements for flow around a sphere in a viscoelastic fluid." *Physics of Fluids*. **11**, 3599-3612 (1999).
- Faroughi, S. A. and C. Huber, "A generalized equation for rheology of emulsions and suspensions of deformable particles subjected to simple shear at low Reynolds number." *Rheologica Acta*. **54**, 85-108 (2015).
- Flatt, R. J., N. Martys and L. Bergstrom, "The rheology of cementitious materials." *Mrs Bulletin*. **29**, 314-318 (2004).
- Foss, D. R. and J. F. Brady, "Brownian Dynamics simulation of hard-sphere colloidal dispersions." *J Rheol*. **44**, 629-651 (2000).
- Fowler, J. N., J. Kirkwood and N. J. Wagner, "Rheology and Microstructure of Shear Thickening Fluid Suspoemulsions." *Applied Rheology*. **24** (2014).

Gadalamaria, F. and A. Acrivos, "Shear-Induced Structure in a Concentrated Suspension of Solid Spheres." *J Rheol.* **24**, 799-814 (1980).

Galindo-Rosales, F. J., F. J. Rubio-Hernandez, A. Sevilla and R. H. Ewoldt, "How Dr. Malcom M. Cross may have tackled the development of "An apparent viscosity function for shear thickening fluids"." *Journal of Non-Newtonian Fluid Mechanics.* **166**, 1421-1424 (2011).

Gauthier, F., H. L. Goldsmith and S. G. Mason, "Particle motions in non-Newtonian media: I. Couette flow." *Rheol Acta.* **10**, 344-364 (1971).

Goff, H. D., "Colloidal aspects of ice cream - A review." *International Dairy Journal.* **7**, 363-373 (1997).

Gurnon, A. K. and N. J. Wagner, "Microstructure and rheology relationships for shear thickening colloidal dispersions." *Journal of Fluid Mechanics.* **769**, 242-276 (2015).

Haddadi, H. and J. F. Morris, "Microstructure and rheology of finite inertia neutrally buoyant suspensions." *Journal of Fluid Mechanics.* **749**, 431-459 (2014).

Highgate, D. J. and R. W. Whorlow, "Rheological properties of suspensions of spheres in non-Newtonian media." *Rheol Acta.* **9**, 569-576 (1970).

Kalman, D. P. *Microstructure and Rheology of Concentrated Suspensions of Near Hard-Sphere Colloids*. PhD Thesis. Ph.D. Thesis University of Delaware (2010).

Karnis, A. and S. G. Mason, "Particle motions in non-Newtonian media." *Trans Soc Rheol.* **10**, 571-592 (1966).

Kataoka, T., T. Kitano, M. Sasahara and K. Nishijima, "Viscosity of particle filled polymer melts." *Rheol Acta.* **17**, 149-155 (1978).

Kulkarni, P. M. and J. F. Morris, "Suspension properties at finite Reynolds number from simulated shear flow." *Physics of Fluids.* **20** (2008).

Laun, H. M., "Rheological Properties of Aqueous Polymer Dispersions." *Angewandte Makromolekulare Chemie.* **123**, 335-359 (1984).

Laun, H. M., "Normal Stresses in Extremely Shear Thickening Polymer Dispersions." *Journal of Non-Newtonian Fluid Mechanics.* **54**, 87-108 (1994).

Le Meins, J. F., P. Moldenaers and J. Mewis, "Suspensions in polymer melts. 1. Effect of particle size on the shear flow behavior." *Industrial & Engineering Chemistry Research.* **41**, 6297-6304 (2002).

Lee, M., M. Alcoutlabi, J. J. Magda, C. Dibble, M. J. Solomon, X. Shi and G. B. McKenna, "The effect of the shear-thickening transition of model colloidal spheres on the sign of N-1 and on the radial pressure profile in torsional shear flows." *J Rheol.* **50**, 293-311 (2006).

- Liard, M., N. S. Martys, W. L. George, D. Lootens and P. Hebraud, "Scaling laws for the flow of generalized Newtonian suspensions." *J Rheol.* **58**, 1993-2015 (2014).
- Lyon, M. K., D. W. Mead, R. E. Elliott and L. G. Leal, "Structure formation in moderately concentrated viscoelastic suspensions in simple shear flow." *J Rheol.* **45**, 881-890 (2001).
- Malkin, A. Y., "Rheology of Filled Polymers." *Advances in Polymer Science.* **96**, 69-97 (1990).
- Mall-Gleissle, S. E., W. Gleissle, G. H. McKinley and H. Buggisch, "The normal stress behaviour of suspensions with viscoelastic matrix fluids." *Rheologica Acta.* **41**, 61-76 (2002).
- Maranzano, B. J. and N. J. Wagner, "The effects of particle size on reversible shear thickening of concentrated colloidal dispersions." *J Chem Phys.* **114**, 10541-10527 (2001).
- Mari, R., R. Seto, J. F. Morris and M. M. Denn, "Shear thickening, frictionless and frictional rheologies in non-Brownian suspensions." *J Rheol.* **58**, 1693-1724 (2014).
- Metzner, A. B., "Rheology of Suspensions in Polymeric Liquids." *J Rheol.* **29**, 739-775 (1985).
- Mewis, J. and R. de Bleyser, "Concentration effects in viscoelastic dispersions." *Rheol Acta.* **14**, 721-728 (1975).
- Mewis, J. and N. J. Wagner. *Colloidal Suspension Rheology*. Cambridge University Press, New York (2012).
- Michele, J., R. Patzold and R. Donis, "Alignment and Aggregation Effects in Suspensions of Spheres in Non-Newtonian Media." *Rheologica Acta.* **16**, 317-321 (1977).
- Mishra, S. K., P. K. Senapati and D. Panda, "Rheological behavior of coal-water slurry." *Energy Sources.* **24**, 159-167 (2002).
- Morris, J. F. and F. Boulay, "Curvilinear flows of noncolloidal suspensions: The role of normal stresses." *J Rheol.* **43**, 1213-1237 (1999).
- Morrison, F. A. *Understanding Rheology*. Oxford University Press, New York (2001).
- Nguyen, Q. D. and D. V. Boger, "Application of rheology to solving tailings disposal problems." *International Journal of Mineral Processing.* **54**, 217-233 (1998).
- Ohl, N. and W. Gleissle, "The Characterization of the Steady-State Shear and Normal Stress Functions of Highly Concentrated Suspensions Formulated with Viscoelastic Liquids." *J Rheol.* **37**, 381-406 (1993).
- Ovarlez, G., S. Rodts, X. Chateau and P. Coussot, "Phenomenology and physical origin of shear localization and shear banding in complex fluids." *Rheologica Acta.* **48**, 831-844 (2009).

Pasquino, R., N. Grizzuti, P. L. Maffettone and F. Greco, "Rheology of dilute and semidilute noncolloidal hard sphere suspensions." *J Rheol.* **52**, 1369-1384 (2008).

Poslinski, A. J., M. E. Ryan, R. K. Gupta, S. G. Seshadri and F. J. Frechette, "Rheological Behavior of Filled Polymeric Systems .1. Yield Stress and Shear-Thinning Effects." *J Rheol.* **32**, 703-735 (1988).

Russel, W. B., D. A. Saville and W. R. Schowalter. *Colloidal Dispersions*. Cambridge University Press, New York (1989).

Russel, W. B., N. J. Wagner and J. Mewis, "Divergence in the low shear viscosity for Brownian hard-sphere dispersions: At random close packing or the glass transition?" *J Rheol.* **57**, 1555-1567 (2013).

Schank, H. M., J. J. M. Slot, R. J. J. Jongschaap and J. Mellema, "The rheology of systems containing rigid spheres suspended in both viscous and viscoelastic media, studied by Stokesian dynamics simulations." *J Rheol.* **44**, 473-498 (2000).

Scirocco, R., J. Vermant and J. Mewis, "Effect of the viscoelasticity of the suspending fluid on structure formation in suspensions." *Journal of Non-Newtonian Fluid Mechanics.* **117**, 183-192 (2004).

See, H., P. Jiang and N. Phan-Thien, "Concentration dependence of the linear viscoelastic properties of particle suspensions." *Rheologica Acta.* **39**, 131-137 (2000).

Shapiro, A. P. and R. F. Probstein, "Random Packings of Spheres and Fluidity Limits of Monodisperse and Bidisperse Suspensions." *Physical Review Letters.* **68**, 1422-1425 (1992).

Shenoy, S. S. and N. J. Wagner, "Influence of medium viscosity and adsorbed polymer on the reversible shear thickening transition in concentrated colloidal dispersions." *Rheol Acta.* **44**, 360-371 (2005).

Shikata, T. and D. S. Pearson, "Viscoelastic Behavior of Concentrated Spherical Suspensions." *J Rheol.* **38**, 601-616 (1994).

Singh, A. and P. R. Nott, "Experimental measurements of the normal stresses in sheared Stokesian suspensions." *Journal of Fluid Mechanics.* **490**, 293-320 (2003).

Slattery, J. C. and R. B. Bird, "Non-Newtonian Flow Past a Sphere." *Chemical Engineering Science.* **16**, 231-241 (1961).

Snijkers, F., G. D'Avino, P. L. Maffettone, F. Greco, M. Hulsen and J. Vermant, "Rotation of a sphere in a viscoelastic liquid subjected to shear flow. Part II. Experimental results." *J Rheol.* **53**, 459-480 (2009).

Tanner, R. I., S. C. Dai, F. Z. Qi and K. Housiadas, "Viscometric functions of semi-dilute non-colloidal suspensions of spheres in a viscoelastic matrix." *Journal of Non-Newtonian Fluid Mechanics*. **201**, 130-134 (2013).

Tanner, R. I., F. Z. Qi and S. C. Dai, "Scaling the normal stresses in concentrated non-colloidal suspensions of spheres." *Rheologica Acta*. **52**, 291-295 (2013).

Toussaint, F., C. Roy and P. H. Jezequel, "Reducing shear thickening of cement-based suspensions." *Rheologica Acta*. **48**, 883-895 (2009).

Wagner, N. J. and A. T. J. M. Woutersen, "The Viscosity of Bimodal and Polydisperse Suspensions of Hard-Spheres in the Dilute Limit." *Journal of Fluid Mechanics*. **278**, 267-287 (1994).

Zapata, P. and J. A. Gambatese, "Energy Consumption of Asphalt and Reinforced Concrete Pavement Materials and Construction." *Journal of Infrastructure Systems*. **11**, 9-20 (2005).

Zarraga, I. E., D. A. Hill and D. T. Leighton, "The characterization of the total stress of concentrated suspensions of noncolloidal spheres in Newtonian fluids." *J Rheol*. **44**, 671-671 (2000).

Zarraga, I. E., D. A. Hill and D. T. Leighton, "Normal stresses and free surface deformation in concentrated suspensions of noncolloidal spheres in a viscoelastic fluid." *J Rheol*. **45**, 1065-1084 (2001).